Soft Matter

The Role of the Molecular Weight of the Adsorbed Layer at a Substrate in the Suppressed Dynamics of Supported Thin Polystyrene Films

Journal:	*Soft Matter*
Manuscript ID	SM-ART-01-2022-000067.R1
Article Type:	Paper
Date Submitted by the Author:	08-Feb-2022
Complete List of Authors:	Ren, Weizhao; Zhejiang Sci-Tech University, Deoartment of Chemistry Wang, Xin; Zhejiang Sci-Tech University, Deoartment of Chemistry Shi, Jiahui; Zhejiang Sci-Tech University, Deoartment of Chemistry Xu, Jianquan; Zhejiang Sci-Tech University, Department of Chemistry Tanaeda, Hidenobu; Kyusyu University, Department of Applied Chemistry Yamada, Norifumi; High Energy Accelerator Research Organisation, Institute of Materials Structure Science Kawaguchi, Daisuke; Kyushu University, Applied Chemistry Tanaka, Keiji; Kyushu University, Applied Chemistry Wang, Xinping; Zhejiang Sci-Tech University, Deoartment of Chemistry

The Role of the Molecular Weight of the Adsorbed Layer at a Substrate in the Suppressed Dynamics of Supported Thin Polystyrene Films†

Weizhao Ren,[a] Xin Wang,[a] Jiahui Shi,[a] Jianquan Xu,*[a] Hidenobu Taneda,[b] Norifumi L. Yamada,[c] Daisuke Kawaguchi,[bd] Keiji Tanaka,*[bd] and Xinping Wang*[a]

[a]Department of Chemistry, Key Laboratory of Surface & Interface Science of Polymer Materials of Zhejiang Province, Zhejiang Sci-Tech University, Hangzhou 310018, P. R. China

E-mail: jqxu@zstu.edu.cn or wxinping@yahoo.com or wxinping@zstu.edu.cn

[b]Department of Applied Chemistry, Kyushu University, Fukuoka, 819-0395, Japan

Email: k-tanaka@cstf.kyushu-u.ac.jp.

[c]Neutron Science Laboratory, High Energy Accelerator Research Organization, 203-1 Shirakata, Tokai, Naka-gun, Ibaraki 319-1106, Japan.

[d]Center for Polymer Interface and Molecular Adhesion Science, Kyushu University, Fukuoka, 819-0395, Japan

†Electronic supplementary information (ESI) available. See DOI: 10.1039/XXXXXXX

ABSTRACT: The adsorbed layer at a solid surface plays a crucial role in the dynamics of nanoconfinement polymer materials. However, the influence of the adsorbed layer is complex, and clarifying this influence on the dynamics of confined polymers remains a major challenge. In this paper, SiO_2-Si substrates with various thicknesses and adsorbed layers of PS with various molecular weights were used to reveal the effect of the adsorbed layer on the corresponding segmental dynamics of supported thin PS films. Strongly suppressed segmental dynamics of thin PS film were observed for the films supported on thicker adsorbed layers or prepared using higher molecular weight. Neutron reflectivity revealed that the overlap region thickness between the adsorbed layer and the top overlayer increased with increasing thickness and molecular weight of the adsorbed layer, both of which correlate well with the distance over which the polystyrene dynamics were depressed by the adsorbed layer. The results show that the influencing distance of the adsorbed layer is related to the overlap zone formed between the adsorption layer and the upper thin film. The effect of the adsorbed layer molecular weight can be ascribed to the fact that large loops and long tails in the adsorbed layer result in stronger interpenetrations and entanglements between polymer chains in the adsorbed layer and in the overlayer, causing a stronger substrate effect and suppression of the segment dynamics of the supported thin PS films.

Keywords: Interface; Adsorbed layer; Polystyrene; Molecular mobility; Overlap region.

1. INTRODUCTION

Due to the exceedingly high specific surface area of polymer nanocomposites and the possibility of controlling the polymer/nanoparticle interfacial interactions, great improvements in the macroscopic properties of nanocomposite materials can be made by adjusting the chain dynamics at these interfaces. It is widely accepted that the interfacial effect plays a crucial role in the resulting physical properties of supported ultrathin polymer films and nanocomposites, with large differences in physical performance observed when different substrates are used.[1-4] For example, an ultrathin poly(methyl methacrylate) film showed a decrease in glass transition temperature (T_g) compared with the bulk T_g when supported by gold substrates, while an increase in T_g resulted when supported by silicon substrates.[1] The T_g of ultrathin PS films could be adjusted by modifying the various aromatic groups anchored on silicon substrate surfaces[3,5] and the loop size of the adsorbed polystyrene (PS) chains.[6,7] In other words, the local relaxation of the chains near the substrate appears to be suppressed by the various interactions between substrate and polymer. Furthermore, the interfacial effect on polymer properties is complex and the nature of the interfacial effect remains unclear. Because an interfacial layer can always be formed near a substrate, it may be the key to a deeper understanding of the interfacial effect.[4,8,9]

Several groups have focused on elucidating the role of a physically adsorbed polymer layer on the T_g of supported thin polymer films.[10-15] It has been suggested that irreversibly adsorbed nanolayers on a substrate, including the corresponding structures and properties, are important to interfacial effects perturbing the dynamics

of thin films. Napolitano *et al.*[15-18] demonstrated the direct relationship between the segmental dynamics in thin polymer films and the degree of chain adsorption at the substrate. The effect of free surface on the T_g of the supported film can be erased by irreversible adsorption. Koga *et al.*[19] and Wang[6,20,21] found that by changing the thickness or structure of the adsorbed layer, the effect of suppressing chain dynamics could propagate to distances of several tens of nanometers away from the substrate.

It has been suggested that the adsorbed layer thickness could be a valuable parameter for evaluating the strength of interfacial interactions. Napolitano *et al.*[10,16] reported that expediting the adsorption of a polymer chain onto the substrate by prolonging annealing time increased the T_g of thin films. They verified that the extent of increase in T_g is proportional to the available free volume at the interface.[10] This was demonstrated by direct experimental evidence,[6] as it was observed that the T_g of thin supported PS films increased linearly with increasing h_{ads}/R_g (h_{ads}, the adsorbed layer thickness on solid substrate; R_g, the radius of gyration of PS). The value h_{ads}/R_g is related to the number and conformation of PS adsorbed chains, with a higher value of h_{ads}/R_g implying a more stretched conformation together with more adsorbed polymer chains existing on the solid substrate.[16] Further, Zuo *et al.*[7] designed adsorbed chains with various loop sizes and indicated that larger loops were more efficient in propagating interfacial effects to the interior region because of the stronger topological constraints between the loops and the upper free chains. Similar results were also reported in a study which found that the distance of the suppressed local dynamics of poly(ethylene terephthalate) from the substrate could be scaled by the

adsorbed layer thickness.[20,22] This effect of adsorbed chains on the dynamics of thin films has usually been attributed to the formation of an overlap zone between the adsorbed layer and the upper free polymer chains, in which the neighboring polymer chains efficiently entangle with the loops of the adsorbed chains and suppress the chain mobility near the solid substrate. The thickness of the overlap region between the bulk-like layer and the adsorbed chains increases with an increase in h_{ads}/R_g, further increasing the propagation distance of the interfacial effect.[7,15,20] Therefore, the nature of the overlap zone is very important in understanding the interfacial effect in nanoconfinement systems and nanocomposite materials. However, few studies have focused on the overlap zone so the relationship between it and the corresponding dynamics of supported thin polymer films is unclear.

It has been reported in previous theoretical works[23] that the adsorbed chains can form loop, train and tail conformations. Recently, Koga *et al.*[24-28] experimentally showed that the adsorbed layer is composed of both a flattened and a loosely adsorbed layer. The thickness of the adsorbed layer depended on the molecular weight and annealing temperature; but the thickness of the flattened layer depended only on the interaction between substrate and segment. In this paper, various thicknesses of a loosely adsorbed PS layer were prepared using various molecular weights of PS and annealing temperatures. The T_g of thin PS films with various thicknesses supported on loosely adsorbed PS layers were investigated. The results showed that the T_g of the PS films were perturbed markedly by the thickness and molecular weight of the adsorbed layer. Direct observation using neutron reflectivity (NR) showed that the thickness of

the overlap zone correlated well with the distance of the interfacial effect propagation.

2. EXPERIMENTAL SECTION

Materials. Monodisperse polystyrenes (*h*PS) with four different molecular weights: PS40 (M_w = 40 kg mol^{-1}, PDI = 1.05); PS222 (M_w = 222 kg mol^{-1}, PDI = 1.06); PS442 (M_w = 442 kg mol^{-1}, PDI = 1.07); PS785 (M_w = 785 kg mol^{-1}, PDI = 1.07) and deuterated polystyrene (*d*PS) (M_w = 252 kg mol^{-1}, PDI = 1.05) were obtained from Polymer Source Inc. (Canada). PS end-capped with 2-perfluorooctylethyl methacrylate (FMA) units (PS_{428}-*ec*-FMA_2, PDI = 1.15) was prepared by atom-transfer radical polymerization (ATRP), as previously described.[29,30]

Preparation of PS adsorbed layers on SiO_2-Si substrates. PS films with various thicknesses were produced by spin-coating toluene solutions of different concentrations onto silicon wafers with a native oxide layer (~2 nm). The spin-cast films (thickness > $8R_g$) were then annealed at 423 K for different times to produce various loosely adsorbed layers. The unadsorbed chains were subsequently leached by toluene according to Guiselin's experiment.[31] The thicknesses of the adsorbed layers were determined by ellipsometry.

Preparation of PS film supported adsorbed layers and their T_g measurements. The PS films supported by adsorbed layers were prepared by spin-coating the toluene solution onto the SiO_2-Si substrates with various thicknesses of the adsorbed layer. Then, the films were annealed under vacuum at 393 K for 24 h.

Fig. S1 (ESI†) shows the T_g and h_{ads} of 60 nm thick PS film supported on 6 nm adsorbed layer with various annealing times (24 h, 48 h and 72 h). It is found that the T_g and h_{ads} are the same within experimental error with different annealing time. Hence, the films annealed at 393 K for 24 h is sufficient to remove residual solvent and equilibrate the film. The T_g values of the equilibrium PS films were determined by ellipsometry (EP^{3}SW, Accurion GmbH Co., Germany) with a heating rate of 2 K min^{-1} and obtained from an inflection point in the normalized thickness vs. T linear correlation, as shown in Fig. S2 (ESI†).

Determination of the propagation distance of the interfacial effect. The diffusion of polymer chains with fluorinated tracer-labeled multilayer films was used to detect the propagation depth of the substrate effect with various adsorbed layers, as in our previous work.[32] The multilayer films were produced by combining spin-coating and floating techniques as previously reported.[33,34] In the present study, the bottom layer is an adsorbed layer of PS. Various thicknesses of PS_{428}-*ec*-FMA_2 layers were then spin-coated with toluene solutions onto the adsorbed layer as the middle layer. To remove the solvent and equilibrate the film, the films were annealed under vacuum at 393 K for 24 h. The upper PS222 layer (about 50 ± 2 nm) was finally obtained by a water-casting method.[35] The multilayer film samples were dried at 323 K for 72 h under vacuum to remove water and the residual solvent. The thickness of each layer was determined by ellipsometry.

X-ray reflectivity (XRR). XRR was used to measure the density distribution of the adsorbed layers by using a Bruker D8 Discover system with a Cu-Kα radiation

source at room temperature. The evolution of the X-ray beam reflectivity with its incident angle (θ) was detected as a reflectivity curve. This curve was fitted by a multilayer model to obtain the mass density profile.

Neutron reflectivity (NR). A Soft Interface Analyzer (SOFIA)[36,37] (BL-16, Materials and Life Science Facility, Japan Proton Accelerator Research Complex (J-PARC), Tokai, Japan) was used for the NR measurements. Neutron beams were guided from the air side into the *d*PS film with a wavelength (λ) of 0.25 to 0.88 nm, and the detection of the reflected beam was performed under specular conditions. Reflectivity was calculated by the function $q = (4\pi/\lambda) \sin \theta$, where θ is the incident angle of the neutrons. Reflectivity was also obtained from the base of the (b/V) profile along the normal direction by the software MOTOFIT.[38] The (b/V) values of SiO_2, *h*PS, and *d*PS were 3.48×10^{-4}, 1.28×10^{-4}, and 6.36×10^{-4} nm^{-2}, respectively.

3. RESULTS AND DISCUSSION

3.1 Effect of substrate with various thicknesses of adsorbed layer on the T_g of supported thin PS films

To investigate the effect of the adsorbed layer on the T_g of the supported thin PS films, substrates with various adsorbed chains were prepared by varying the annealing temperature and the molecular weight of PS. Fig. S3 (ESI†) shows that the equilibrium thickness of the adsorbed layer was about $0.67R_g$, which is molecular weight independent. The XRR profile of a 10.9 nm-thick adsorbed layer for PS442 shown in Fig. S4a (ESI†) confirmed this two-layer structure. These findings are in

agreement with those previously reported.[26-28] Concurrently, Fig. S4b (ESI†) shows that the surface of the adsorbed layer is homogeneous. In this paper, such adsorbed layers were used as substrates for the supported thin PS films.

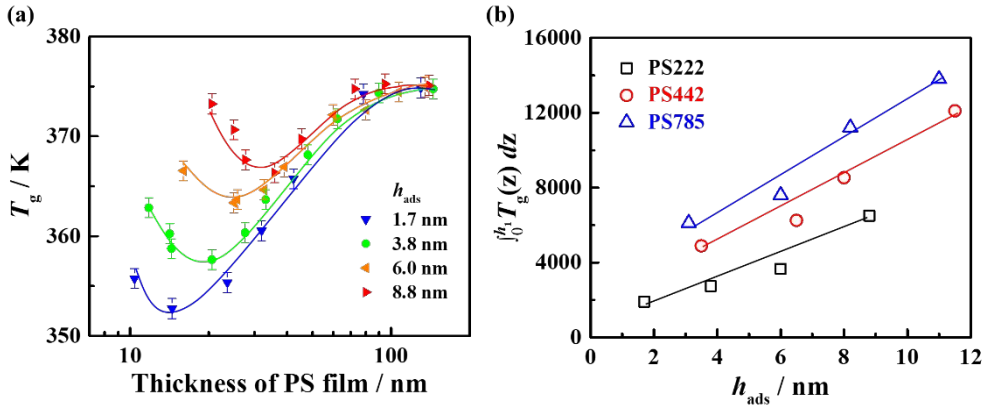

Fig. 1 (a) Thickness dependence of T_g for PS222 films supported on adsorbed layers with various h_{ads}. The solid curves are the best fits obtained by Equation (1). (b) The relationship between $\int_0^{h_1} T_g(z)dz$ and h_{ads} for PS222, PS442 and PS785 films.

The T_g of PS222 films supported on adsorbed layers with various thicknesses are presented in Fig. 1a. The results indicate that the T_g first decreased and then increased with reducing film thickness. This was different behavior from that observed for the PS film supported on neat SiO_2 (Fig. S5, ESI†) which monotonously decreased with decreasing film thickness, as previously reported.[1] A critical thickness (h^*) was defined as the inflection point of the curve, below which the T_g showed the lowest value. This phenomenon was also observed for PS-COOH on an SiO_2 substrate[39,40] and PS supported on an adsorbed layer with various sizes of loops.'[7] The authors of these previous studies attributed this phenomenon to the T_g of the films first decreasing due to a dominating free surface effect and then increasing due to a dominating interfacial effect.[41,42] The critical thickness h^* clearly represents the

transition from domination of the surface effect to interfacial effect, and T_g^*, defined as T_g at h^*, increased with increasing thickness of the adsorbed layer. The larger h^* and higher T_g^* indicate that the thicker adsorbed layer enhances the interfacial effect of the supported PS film. Based on a three-layer model, the contribution of interfacial effects on T_g of the supported PS films could be identified by fitting the curve of $T_g(h)$ with film thickness using Eq. (1).[1,7,43]

$$T_g(h) = \frac{h - h_1}{h} T_g^{bulk}\left[1 - \left(\frac{\gamma}{h}\right)^{\delta}\right] + \frac{\int_0^{h_1} T_g(z)dz}{h} \quad (1)$$

The $T_g(h)$ value includes the contribution of a free surface layer, a bulk layer and an interfacial layer. In Eq. (1), the first term describes the effect of the free surface. For a PS film, the free surface-related parameters γ and δ are 3.2 ± 0.6 nm and 1.8 ± 0.6, respectively.[1,43] The second term in Eq. (1) is the contribution of the suppressed interfacial dynamics to the T_g of the whole film. $T_g(z)$ are the local T_g values at different locations in the interfacial layer. $\int_0^{h_1} T_g(z)dz$ is the sum of $T_g(z)$ of all of the interfacial layers at various distances from the adsorbed layer and is a very effective parameter for scaling the interfacial effect, in which h_1 is the thickness of the interfacial layers. Fig. 1b shows that $\int_0^{h_1} T_g(z)dz$ increases with increasing thickness of the adsorbed layer (h_{ads}). This result shows that the suppressed interfacial dynamics were reinforced by increasing h_{ads}. According to the results obtained from the adsorbed layers on the SiO_2-Si substrate from PS films with various thicknesses as shown in Fig. S6 (ESI†), the observed monotonous decrease with thickness of the T_g of the PS films on neat silicon substrates was attributed to the weak interfacial effect caused by the thinner adsorbed layer when the thickness of PS film became much

thinner.

The effect of the molecular weight of the adsorbed layer on the T_g of the thin PS films was also investigated. The $\int_0^{h_1} T_g(z)dz$ values of PS films supported on adsorbed layers with PS442 and PS785 obtained from the data shown in Fig. S7 (ESI†) are presented in Fig. 1b. Similarly, the results suggest that the suppressed interfacial dynamics were reinforced by the thicker adsorbed layer. The correlation between the integral term in Eq. (1) and the molecular weight of an adsorbed layer with a similar thickness was plotted and is presented in Fig. 2. It was found that $\int_0^{h_1} T_g(z)dz$ increased with increasing molecular weight at a given h_{ads}. This result indicates that the molecular weight of the adsorbed layer also plays a key role in the dynamics of supported polymer films except for the thickness of the adsorbed layer. The suppressed interfacial dynamics could thus accordingly be reinforced by increasing the molecular weight of the adsorbed layer.

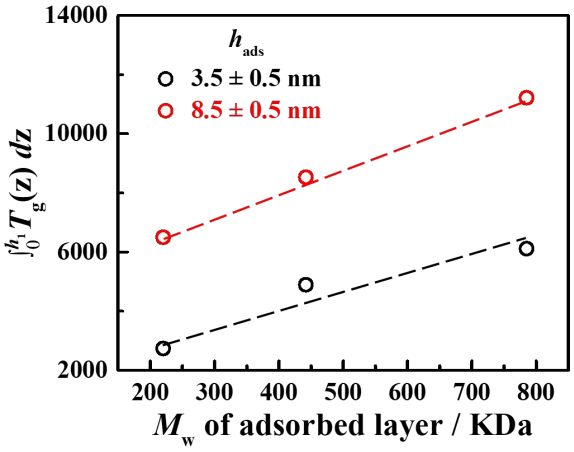

Fig. 2 Contribution of interfacial effects $\int_0^{h_1} T_g(z)dz$ as a function of molecular weight of the adsorbed layer. PS222 was used as the supported thin film.

Most reports[6,7,16,20] have indicated that with increasing h_{ads}, the segmental dynamics were severely perturbed in polymer films. Both Napolitano[16] and Wang[6] revealed a linear relationship between h_{ads} and T_g. Napolitano *et al*.[15] reported that the h_{ads} increased with annealing time, leading to a limitation or even total elimination of the free surface effect. The increases of T_g linearly relate to the degree of adsorption, which was attributed to the decrease of the free volume at the interfacial regions. Glynos *et al*.[44] found this to be the case for, independently, either the molecular weight or the functionality of the arms in the case of star-shaped chains, which confirmed the validity of this relationship. However, it is interesting that the molecular weight of the adsorbed layer has an obvious effect on the T_g of the supported PS films. To obtain a better understanding of the effect of the molecular weight of the adsorbed layer, the distance of segmental mobility suppressed by the adsorbed layer was investigated.

3.2 Effect of the adsorbed layer with various M_w on the propagation distance of the interfacial effect

It is well accepted that the interfacial effect is a long-range effect. Therefore, the propagation distance is very important and could be regarded as a key parameter for perturbing the dynamics of the films. We next focus on the propagation distance of PS chains dynamics suppressed by the adsorbed layer using a fluorinated tracer-labeled method.[32] A typical multilayer film as shown in Fig. 3a was fabricated, consisting of a bottom adsorbed PS layer, a middle layer with a variable thickness PS_{428}-*ec*-FMA_2,

and an upper layer of PS222 (50 ± 2 nm). Upon annealing at 403 K (T_g^{bulk}+ 30 K), the PS_{428}-*ec*-FMA_2 chains diffused from the middle layer to the free surface, resulting in an increase in water contact angle (CA) as previously reported.[32] The critical time (t^*) needed for the PS_{428}-*ec*-FMA_2 chains to reach the top surface was obtained from the intersection of two straight lines, as shown in Fig. 3b. It is worth noting that the value of t^* is usually obtained within 1 h, which is really short that the growth of adsorbed layer can be ignored even at 423 K, see Fig. S3 (ESI†). Fig. 3c shows the relationship between the thickness of the PS_{428}-*ec*-FMA_2 layer (h_{mid}) and the critical time (t^*) with various adsorbed layers.

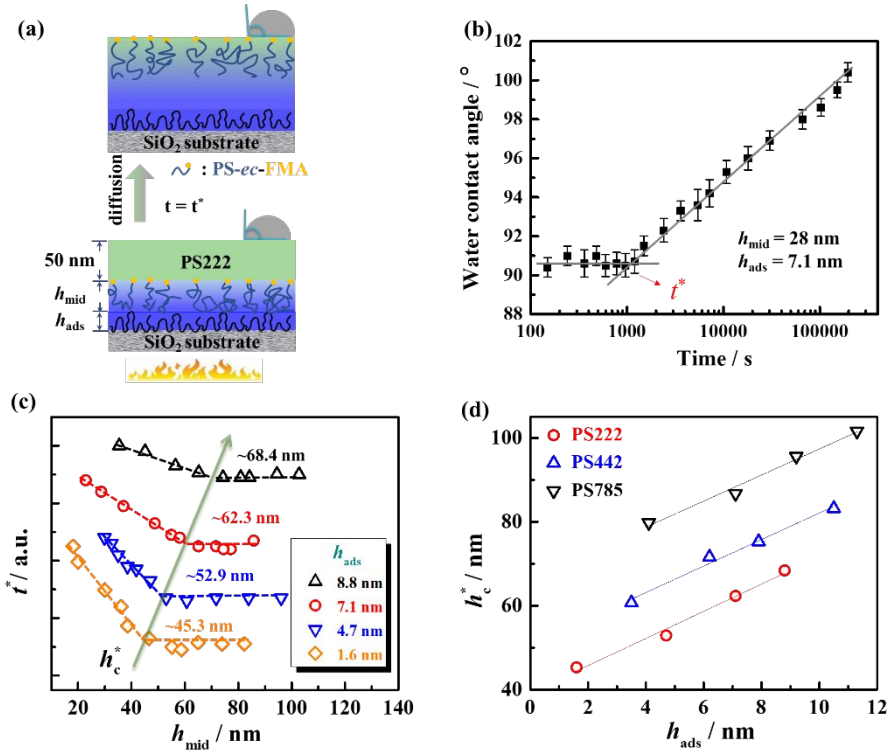

Fig. 3 (a) Schematic of a multilayer film sample and the diffusion of the PS_{428}-*ec*-FMA_2. (b) The evolution of water contact angles (CA) on the surface of a multilayer film with annealing time at 403 K. (c) Relationship between the critical time (t^*) and the thickness of the middle layer (h_{mid}) in multilayer films on the adsorbed layer. The molecular weight of the adsorbed layer was 222 kg/mol. (d) Relationship between h_c^* and the thickness of adsorbed layer on the substrate for PS222, PS442 and PS785 (T = 403 K).

It is apparent that the t^* value increased as the h_{mid} decreased at $h_{mid} < h_c^*$, due to the increasing influence of the adsorbed layer on chain mobility near the substrate. In contrast, when $h_{mid} > h_c^*$, the chain mobility of the labeled PS at the interface was not affected by the adsorbed layer, thereby leading to a constant t^* value. Accordingly, the propagation distance of the interfacial effect could be marked as h_c^*, as verified previously.[32] It was observed that the value of h_c^* was approximately 45.3 nm to 68.4 nm, with the thickness of the adsorbed layer changing from 1.6 nm to 8.8 nm. Fig. 3d presents h_c^* values for various thicknesses of the adsorbed layer prepared by PS with M_w of 222, 442 and 785 kg/mol, respectively. It may be observed that h_c^* increased linearly with increasing thickness of the adsorbed layer (h_{ads}). Interestingly, h_c^* was dependent on the molecular weight of the adsorbed layer. At the same thickness of adsorbed layer, the h_c^* increased with increasing M_w. Additionally, the slopes from the relationship between h_c^* and h_{ads} were the same for the films with different M_w. By comparing Fig. 1b and Fig. 3d, it is clear that the integral term $\int_0^{h_1} T_g(z)dz$, namely the contribution of the suppressed interfacial dynamics, was related to h_c^*. That is, h_c^* values indicate that the substrate effect propagated to a greater distance from the substrate. The data shown in Figs. 2 and 3d indicate that the molecular weight dependence of the integral term at the same h_{ads} is attributed to h_c^*, whereby higher molecular weights of the adsorbed layer present a longer influencing distance suppressed by the adsorbed layer. The results of our previous reports[6,7,20] in which the suppressed T_g of supported polymer films and h_c^* were only related to h_{ads}/R_g, are

different from the results shown in Fig. 1b and Fig. 3d. This difference may be attributed to the complicated structure of the adsorbed layer. In the current study, the adsorbed layer did not a reach a "quasiequilibrium" state. This factor will be studied more closely in our next work.

In our previous work, h_c^* was adjusted by changing the loop size of the adsorbed chain at the substrate[20] and the phenyl group content on a phenyl group-modified substrate.[2] The interface-induced PS viscosity and T_g increased linearly with the distance of chain mobility suppressed by the substrate.[2,7] Zuo[7] and Bram[45] found that strong interpenetrations between the adsorbed layer and the free chains in the film impacted thin film dynamics. It is reasonable to suggest that the adsorbed layer entangles with free chains, affecting h_c^* and suppressing the dynamics of the supported film. Therefore, we next discuss how the interpenetration region impacts h_c^* and the segmental dynamics. At the same time, we try to clarify the mechanism of the dependence of the molecular weight of the adsorbed layer on both h_c^* and the segmental dynamics of supported PS films.

3.3 Mechanism of the T_g of thin PS film supported on substrates with various adsorbed layers

Dewetting experiments are extremely sensitive methods for investigating polymer/solid interfacial interactions, such as the friction coefficient,[46,47] and depth of interpenetration.[46] Due to the difficulty in observation of dewetting for overlayer PS film with high molecular weight, PS40 with a relatively low molecular weight was

used as a supported thin PS film (about 45 nm) atop a PS adsorbed layer. Fig. S8 (ESI†) shows that the dewetting behavior was suppressed with an increase in both the thickness and M_w of the adsorbed layer. These observations are similar to Jiang's report that a high M_w adsorbed layer made the PS overlayer more stable (not dewetting) compared to a low M_w layer.[28] They attributed this phenomenon to the fact that long chains in the adsorbed layer penetrate into the overlayer to form a thick overlap zone. The dewetting result conforms to the relationship between the propagation distance of the interfacial effect and the thickness or molecular weight of the adsorbed layer.

NR measurements using deuterated polymer were conducted to study the interpenetration region between the adsorbed chains and the upper layer free chains. A *d*PS (M_w = 252 kg mol^{-1}, PDI = 1.05) overlayer (about 45 nm) was prepared on the adsorbed layer, and the interpenetration process was examined at room temperature. Fig. 4a shows the typical NR results for the 45 nm thick *d*PS films supported on adsorbed layers with various thicknesses prepared by PS222 and annealed at 393 K for 24 h. Fig. 4b shows the scattering length density (*b*/*V*) profiles of the films which gave the best-fit reflectivity. The fitting parameters are presented in Table S1 (ESI†). The (*b*/*V*) values of the adsorbed molecules *h*PS and top layer *d*PS were about 1.28×10^{-4} nm^{-2} and 6.36×10^{-4} nm^{-2} respectively as shown in Fig. S9b (ESI†). As *h*PS in the adsorbed layer penetrated into the top *d*PS films, the (*b*/*V*) value close to the substrate would decrease. From Fig. 4b, it is clear that the *d*PS chains could interpenetrate into the adsorbed layer reaching to the SiO_2-Si surface (i.e., $b/V_{(z=0)}$ =

3.5×10^{-4} nm^{-2}) regardless of the thickness of the adsorbed layer (h_{ads}). This phenomenon also means that the adsorbed layer is not "frozen" during annealing. Furthermore, the interfacial width in which region the (b/V) value was lower than 6.36×10^{-4} nm^{-2} and higher than 1.28×10^{-4} nm^{-2} broadened with an increase in h_{ads}, thus increasing the entropy of the free chains in this way. Thus, it is reasonable that this interfacial width can be considered as an overlap region (h^{OR}) in which the *h*PS chains in the adsorbed layer and *d*PS chains in the top films penetrated each other. At the same time, it is clear from the data in Fig. 4b and Table S1 (ESI†) that h^{OR} increased with increasing thickness of the adsorbed layer (h_{ads}).

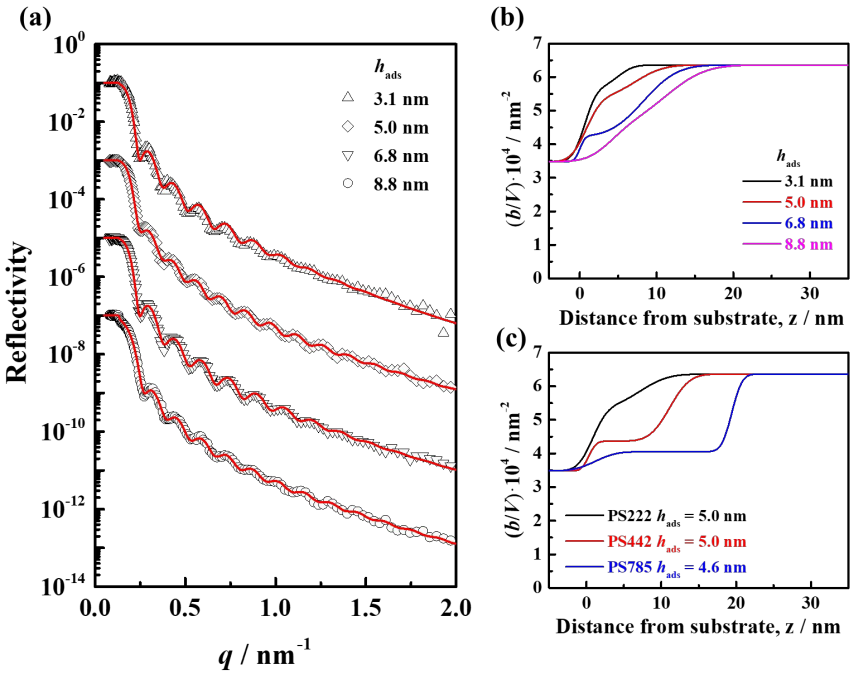

Fig. 4 (a) NR profiles of ~45 nm thick *d*PS films supported on an adsorbed layer with various thicknesses prepared by PS222. Open symbols and solid lines represent the experimental data and the best fits to the NR profiles, respectively. (b) (b/V) profiles of ~45 nm thick *d*PS films supported on PS adsorbed layers with various thicknesses annealed at 393 K for 24 h. (c) (b/V) profiles of *d*PS films supported on a PS adsorbed layer of about 5.0 nm prepared by PS222, PS442 and PS785 annealed at 393 K for 24 h.

To understand the effect of the molecular weight of the adsorbed layer, the thicknesses of the overlap region (h^{OR}) for adsorbed layers prepared from PS442 and PS785 were investigated using NR and the results are presented in Fig. S10 (ESI†) and Table S2 (ESI†). It is clear from the data shown in Fig. 4c that the thicknesses of the overlap region (h^{OR}) increased with the increase of the adsorbed layer molecular weight at similar h_{ads}. When the value of h_{ads} was about 5.0 nm, h^{OR} was 13.0 nm (0.992 R_g), 16.8 nm (0.908 R_g) and 22.3 nm (0.906 R_g), corresponding to 222 kg/mol, 442 kg/mol and 785 kg/mol of M_w of adsorbed layer, respectively. This result suggests that the thickness of the overlap region is related to the size of the polymer of the adsorbed layer, revealing that both an increase in thickness and M_w of the adsorbed layer may result in an increase in the overlap region (h^{OR}) between the adsorbed layer and the PS overlayer on top of the adsorbed layer.

In Fig. 5a, the h^{OR} (from Tables S1 and S2, ESI†) is plotted against M_w for PS adsorbed layers with similar h_{ads} and h_{ads}/R_g. The h^{OR} increased with increasing M_w of the adsorbed layer. Fig. 5b shows that both h_c^* and $\int_0^{h_1} T_g(z)dz$ increased linearly with increasing h^{OR}. The data for the thickness of the overlap region for various molecular weights of adsorbed layers collapsed to a straight line. These results clearly demonstrate that the propagation distance of the influence of the adsorbed layer of thin PS films can be scaled by the overlap region of the suppressed interfacial dynamics. These results help to clarify the interfacial effects of confined polymers, i.e., the effect of the adsorbed layer varies with M_w and thickness, which can be

combined with the thickness of the overlap region.

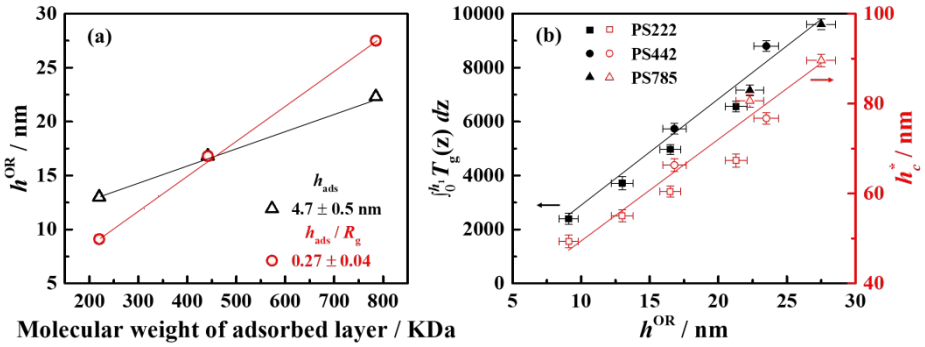

Fig. 5 (a) Thickness of overlap region (h^{OR}) between *h*PS adsorbed layer with various molecular weights and *d*PS top film obtained from NR data fitting results. (b) Dependence on h^{OR} of h_c^* and $\int_0^{h_1} T_g(z)dz$.

The effects of the molecular weight and thickness of the adsorbed layer on the T_g of supported thin PS films can be described by the concept of ‘‘connector molecules’’ as reported by de Gennes[48] and verified by Reiter *et al.*[47,49] The latter found that long grafted bush chains (as the “connectors”) strongly suppressed dewetting in bilayers. This observation was attributed to the mechanism whereby the other end of the brushes act as a connector and penetrate into the upper layer in order to regain their equilibrium Gaussian conformation, thereby aiding the connector pull-out forces.[47,50] The PS adsorbed layer on the substrate surface consisting of high molecular weight[28] or larger loops[7] were reported to be preferable for forming a stable interface between the adsorbed chains and the free polymer layer interface or to improve their adhesion. The improved stabilization overlayer may be attributed to the long-grafted molecules and large loop sizes of the adsorbed layer acting as the connectors easily forming stronger interpenetrations between molecules in the adsorbed layers and the free

chains in the film.[46,47,50]

It is widely reported both from theoretical and experimental approaches[26,31,51] that the conformations of polymer chains adsorbed onto a substrate can be described by a "loop-train-tail" model.[52] Here, loops and trains are polymer segments contacting either directly or not contacting the solid substrate at all, respectively, and the tails are chain ends which not do contact the surface. This model provides a precise balance between the attractive polymer chains and the surface[53] and reflects the conformational and translational entropy loss caused by the immobilization of a polymer chain adsorbed on the substrate surface. It has been widely reported[24-26] that the adsorbed layer consists of flattened chains (i.e., a flattened layer) and loosely adsorbed chains. Before reaching the "quasiequilibrium" state, the thicknesses of the flattened layer and the loosely adsorbed layer increased with increasing annealing time.[25,26] During this process, the number of trains in the adsorbed chain increased and the numbers of loops and tails in the adsorbed chains consequently decreased. Since the adsorbed layers used in this study were mostly in a "pre-quasiequilibrium" state, many of the adsorbed chains thereby existed in the loops and tails conformations. Therefore, in this experiment, the observed increases in adsorbed layer thickness and molecular weight may have been caused by the increasing numbers of large loops and long tails in the adsorbed chains on the solid substrate surface and in the loosely adsorbed chains on its top surface. For similar h_{ads} and high molecular weight, the adsorbed layer contains a relatively low amount of adsorbed polymer chains which consist of relatively large loops and long tails, with few direct contacts with the solid surface. Daoulas *et al.*[54,55] reported that the equilibrium conformations of polyethylene adsorbed molecules were further characterized by considering the properties of tails, loops, and trains, as derived by self-consistent field analysis from

the two coarse-grained models and from the atomistic simulations. It is found that with increasing the chain length in adsorbed layer, the number of tail and loop chains increase while the proportion of trains decreases. According to the explanation proposed by de Gennes,[56] the dynamic character can be transmitted from one part of the chain to another part. Experimentally, surface-enhanced interfacial slippage[57] and an increase in effective viscosity, η_{eff}, were previously observed for PS films with similar thickness to R_g treated by UVO[58] due to the chain connectivity on the substrate surface. Roth *et al*.[59] also found that for PS chains adjacent to the PS-grafted chains, the chain connectivity played an important role in T_g perturbation over a wide range (~ 100 nm). In our previous report,[60] the weak molecular weight dependence of the T_g for PS single chains end-grafted on the substrate was observed, indicating that the lower mobility character of segments around the grafted point may be transferred to other parts along the polymer chain owing to the connectivity between substrate and end-tethering chains. Therefore, the results in this paper could be explained as follows. The distance of segment mobility suppressed by the adsorbed layer was dominated by the length of the loops and tails in the adsorbed chains on the substrate and the loose chains on the top. When the adsorbed layer was prepared by PS with high molecular weight, a thicker overlapped region was formed due to long tails and large loops in the adsorbed layer, resulting in a long influencing distance of the substrate effect. This is similar to the results reported for PS thin films supported on short and long grafted brush blends, with the long brushes serving as the connectors, resulting in a large interfacial region.[49] This is why both the distance of the polymer dynamic suppression from the substrate (h_c^*) and the thickness of the overlap zone increased with increasing PS molecular weight in the adsorbed layer. At the same time, the interpenetrations and entanglements between chains in the adsorbed layers

and the free chains in the overlayer resulted in a substrate effect and suppression of the segmental dynamics of the supported thin PS films.

4. CONCLUSIONS

This paper provides a new insight into the interfacial effects on the segmental dynamics of nanoconfined polymers. It was found that the thickness and molecular weight of polymer adsorbed chains atop the substrate have a key effect on the propagation of suppressed dynamics. The adsorbed chains with greater thickness are more efficient because of the formation of a thicker overlap region with free chains, which allows the interfacial effects to be propagated far from the substrate. At a given h_{ads}, the distance to which the interfacial effect propagates became longer with increasing M_w. Accordingly, the T_g of supported PS film was enhanced by the molecular weight of the adsorbed layer. The reason for this enhancement was attributed to the influencing distance being determined by the overlapped zone in which the adsorbed layer with high molecular weight has long tails resulting in a thicker overlapped zone, which ultimately causes stronger suppression of the corresponding segment dynamics of supported thin polymer films. These findings allow us to use the rationalized design of the adsorbed layer to manipulate the propagation distance of interfacial effects, and more precisely, the height and M_w of the adsorbed layer. These results thus have strong implications for controlling the film stability and have considerable potential for the future design of polymer nanocomposites.

Conflicts of interest

The authors declare no competing financial interest.

Acknowledgements

We are thankful for financial support from the National Natural Science Foundation of China (Nos. 21873085, 22173081 and 22161160317) and from the JST-Mirai Program (JPMJMI18A2). NR measurements were performed on the BL-16 at the Materials and Life Science Facility, J-PARC, Japan under program Nos. 2017L2501 and 2019I1608.

REFERENCES

1 J. L. Keddie, R. A. L. Jones and R. A. Cory, *Faraday Discuss.*, 1994, **98**, 219-230.

2 B. Zuo, F. Wang, Z. Hao, H. He, S. Zhang, R. D. Priestley and X. Wang, *Macromolecules*, 2019, **52**, 3753-3762.

3 Y. Hong, Y. Li, F. Wang, B. Zuo, X. Wang, L. Zhang, D. Kawaguchi and K. Tanaka, *Macromolecules*, 2018, **51**, 5620-5627.

4 A. P. Holt, V. Bocharova, S. Cheng, A. M. Kisliuk, B. T. White, T. Saito, D. Uhrig, J. P. Mahalik, R. Kumar, A. E. Imel, T. Etampawala, H. Martin, N. Sikes, B. G. Sumpter, M. D. Dadmun and A. P. Sokolov, *ACS Nano*, 2016, **10**, 6843-6852.

5 Y. Hong, W. Chen, H. Fang, B. Zuo, Y. Yuan, L. Zhang and X. Wang, *J. Phys. Chem. C.*, 2019, **123**, 19715-19724.

6 S. Sun, H. Xu, J. Han, Y. Zhu, B. Zuo, X. Wang and W. Zhang, *Soft Matter*, 2016, **12**, 8348-8358.

7 B. Zuo, H. Zhou, M. J. B. Davis, X. Wang and R. D. Priestley, *Phys. Rev. Lett.*, 2019, **122**, 217801.

8 D. S. Fryer, R. D. Peters, E. J. Kim, J. E. Tomaszewski, J. J. de Pablo and P. F. Nealey, *Macromolecules*, 2001, **34**, 5627-5634..

9 J. A. Torres, P. F. Nealey and J. J. de Pablo, *Phys. Rev. Lett.*, 2000, **85**, 3221-3224.

10 S. Napolitano, C. Rotella and M. Wübbenhorst, *ACS Macro Lett.*, 2012, **1**, 1189-1193.

11 C. Rotella, S. Napolitano, S. Vandendriessche, V. K. Valev, T. Verbiest, M. Larkowska, S. Kucharski and M. Wübbenhorst, *Langmuir*, 2011, **27**, 13533-13538.

12 H. Yin, S. Napolitano and A. Schönhals, *Macromolecules*, 2012, **45**, 1652-1662.

13 S. Napolitano, S. Capponi and B. Vanroy, *Eur. Phys. J. E: Soft Matter Biol. Phys.*, 2013, **36**, 61.

14 M. J. Burroughs, S. Napolitano, D. Cangialosi and R. D. Priestley, *Macromolecules*, 2016, **49**, 4647-4655.

15 N. G. Perez-de-Eulate, M. Sferrazza, D. Cangialosi and S. Napolitano, *ACS Macro Lett.*, 2017, **6**, 354-358.

16 S. Napolitano and M. Wübbenhorst, *Nat. Commun.*, 2011, **2**,260.

17 A. Panagopoulou and S. Napolitano, *Phys. Rev. Lett.*, 2017, **119**, 097801.

18 D. N. Simavilla, W. Huang, C. Housmans, M. Sferrazza and S. Napolitano, *ACS Cent. Sci.*, 2018, **4**, 755-759.

19 T. Koga, N. Jiang, P. Gin, M. K. Endoh, S. Narayanan, L. B. Lurio and S. K. Sinha, *Phys. Rev. Lett.*, 2011, **107**, 225901.

20 J. Xu, Z. Liu, Y. Lan, B. Zuo, X. Wang, J. Yang, W. Zhang and W. Hu, *Macromolecules*, 2017, **50**, 6804-6812.

21 B. Zuo, J. Xu, S. Sun, Y. Liu, J. Yang, L. Zhang and X. Wang, *J. Chem. Phys.*, 2016, **144**, 234902.

22 X. Wu, J. Xu, W. Sun, Y. Hong, C. Zhang, L. Zhang and X. Wang, *Macromolecules*, 2020, **53**, 8683-8692.

23 K. Motomura and R. Matuura, *J. Chem. Phys.*, 1969, **50**, 1281-1287.

24 P. Gin, N. Jiang, C. Liang, T. Taniguchi, B. Akgun, S. K. Satija, M. K. Endoh and T. Koga, *Phys. Rev. Lett.*, 2012, **109**, 265501.

25 N. Jiang, J. Shang, X. Di, M. K. Endoh and T. Koga, *Macromolecules*, 2014, **47**, 2682-2689.

26 C. Housmans, M. Sferrazza and S. Napolitano, *Macromolecules*, 2014, **47**, 3390-3393.

27 N. Jiang, L. Sendogdular, X. Di, M. Sen, P. Gin, M. K. Endoh, T. Koga, B. Akgun, M. Dimitriou and S. Satija, *Macromolecules*, 2015, **48**, 1795-1803.

28 N. Jiang, J. Wang, X. Di, J. Cheung, W. Zeng, M. K. Endoh, T. Koga and S. K. Satija, *Soft Matter*, 2016, **12**, 1801-1809.

29 J. Yang, D. Yuan, B. Zhou, J. Gao, H. Ni, L. Zhang and X. Wang, *J. Colloid Interface Sci.*, 2011, **359**, 269-278.

30 H. Ni, X. Li, Y. Hu, B. Zuo, Z. Zhao, J. Yang, D. Yuan, X. Ye and X. Wang, *J. Phys. Chem. C.*, 2012, **116**, 24151-24160.

31 O. Guiselin, *Europhys. Lett.*, 1992, **17**, 225-230

32 J. Xu, Y. Zhang, H. Zhou, Y. Hong, B. Zuo, X. Wang and L. Zhang, *Macromolecules*, 2017, **50**, 5905-5913.

33 C. J. Ellison and J. M. Torkelson, *Nat. Mater.*, 2003, **2**, 695-700.

34 J. Kraus, P. M. Buschbaum, D. G. Bucknall, M. Stamm, *J. Polym. Sci., Part B: Polym. Phys.*, 1999, **37**, 2862-2874.

35 X. Zheng, M. H. Rafailovich, J. Sokolov, Y. Strzhemechny, S. A. Schwarz, B. B. Sauer and M. Rubinstein, *Phys. Rev. Lett.*, 1997, **79**, 241-244.

36 N. L. Yamada, N. Torikai, K. Mitamura, H. Sagehashi, S. Sato, H. Seto, T. Sugita, S. Goko, M. Furusaka, T. Oda, M. Hino, T. Fujiwara, H. Takahashi and A. Takahara, *Eur. Phys. J. Plus.*, 2011, **126**, 108.

37 K. Mitamura, N. L. Yamada, H. Sagehashi, N. Torikai, H. Arita, M. Terada, M. Kobayashi, S. Sato, H. Seto, S. Goko, M. Furusaka, T. Oda, M. Hino, H. Jinnai and A. Takahara, *Polym. J.*, 2012, **45**, 100-108.

38 A. Nelson, *J. Appl. Crystallogr.*, 2006, **39**, 273-276.

39 J. L. Keddie and R. A. L. Jones, *Isr. J. Chem.*, 1995, **35**, 21-26.

40 J. A. Forrest and J. Mattsson, *Phys. Rev. E.*, 2000, **61**, R53-R56.

41 M. Campoy-Quiles, M. Sims, P. G. Etchegoin and D. D. C. Bradley, *Macromolecules*, 2006, **39**, 7673-7680.

42 D. Liu, R. Osuna Orozco and T. Wang, *Phys. Rev. E Stat. Nonlin. Soft Matter Phys.*, 2013, **88**, 022601.

43 J. L. Keddie, R. A. L. Jones and R. A. Cory, *Europhys. Lett.*, 1994, **27**, 59-64.

44 E. Glynos, B. Frieberg, A. Chremos, G. Sakellariou, D. W. Gidley and P. F. Green, *Macromolecules*, 2015, **48**, 2305-2312.

45 B. Vanroy, M. Wübbenhorst and S. Napolitano, *ACS Macro Lett.*, 2013, **2**, 168-172.

46 G. Reiter and R. Khanna, *Phys. Rev. Lett.*, 2000, **85**, 2753-2756.

47 G. Reiter, J. Schultz, P. Auroy and L. Auvray, *Europhys. Lett.*, 1996, **33**, 29-34.

48 E. Raphael and P. G. de Gennes, *J. Phys. Chem.*, 1992, **96**, 4002-4007.

49 G. Reiter, P. Auroy and L. Auvray, *Macromolecules*, 1996, **29**, 2150-2157.

50 G. Reiter, A. Sharma, A. Casoli, M. O. David, R. Khanna and P. Auroy, *Langmuir*, 1999, **15**, 2551-2558.

51 P. G. de Gennes, *Macromolecules*, 1980, **13**, 1069-1075.

52 E. Jenckel and B. Rumbach, Z. Elektrochem. *Angew. Phys. Chem.*, 1951, **55**, 612-618.

53 G. J. Fleer, M. A. cohen stuart, J. M. H. M. Scheutjens, T. Cosgrove and B. Vincent, *Polymers at Interfaces,* Chapman & Hall, London, UK 1993.

54 K. C. Daoulas, V. A. Harmandaris and V. G. Mavrantzas, *Macromolecules*, 2005, **38**, 5780-5795.

55 K. C. Daoulas, D. N. Theodorou, V. A. Harmandaris, N. C. Karayiannis and V. G. Mavrantzas, *Macromolecules*, 2005, **38** , 7134-7149.

56 P. G. de Gennes, *Eur. Phys. J. E.*, 2000, **2**, 201-205.
57 F. Chen, D. Peng, C.-H. Lam and O. K. C. Tsui, *Macromolecules*, 2015, **48**, 5034-5039.
58 X. Yu, P. Yiu, L.-T. Weng, F. Chen and O. K. C. Tsui, *Macromolecules*, 2019, **52**, 877-885.
59 X. Huang and C. B. Roth, *ACS Macro Lett.*, 2018, **7**, 269-274.
60 Y. Li, D. Lin, J. Xu, X. Zhou, B. Zuo, O. K. C. Tsui, W. Zhang and X. Wang, *J. Chem. Phys.*, 2020, **152**, 064904.